Tuning the Spin-Crossover Properties
of the $[(Cp^{1-R})_2Mn]$ Metallocenes

Florian Matz[1] and Jordi Cirera[2],*

[1] Institut für Physikalische Chemie und Elektrochemie, Callinstraße 3A,

30167 Hannover, Germany

[2] Departament de Química Inorgànica i Orgànica and

Institut de Recerca de Química Teòrica i Computacional, Universitat de Barcelona,

Diagonal 645, 08028 Barcelona, Spain

Email corresponding author: jordi.cirera@qi.ub.es

Abstract

In this work, we present a computational study using density functional theory (DFT) on how the single functionalization of the cyclopentadienyl ligand in $[(Cp^{1-R})_2Mn]$ systems can be used to tune the spin-crossover properties in such systems. Using the OLYP functional, accurate values for the transition temperature ($T_{1/2}$) can be obtained, and our DFT methodology can be used to explore the effect that different substituents have on tuning such quantity. In particular, we show that the electronic structure of the $[(Cp^{1-R})_2Mn]$ can be tuned via the R group, allowing for a fine-tuning degree of the $T_{1/2}$ that expands between 0 and 400 K. Our results allow for a rational design of new manganocene based systems with tailored SCO properties.

1. Introduction

Spin-crossover (SCO) systems are molecules or materials that can switch between two alternative spin-states, thus exhibiting switching behaviour.[1-4] The transition from the low- to the high-spin state can be triggered using an external stimulus, commonly temperature, and with the spin-state change there are profound changes in the physical properties of the system. This duality is very appealing from the technological point of view, because one can envision harvesting such materials for molecular level devices or spintronic applications.[5-8] The SCO phenomenon, firstly reported nearly a century ago,[9] has grown at the interface between physics and chemistry, and the number of compounds exhibiting SCO behaviour has vastly increased over the last years. Despite the large development of the field, the vast majority of systems exhibiting SCO behaviour contain an Fe^{II} (d^6) metal center,[10-14] and there is an increasing interest on expanding the set of compounds with other metals and oxidation states exhibiting this behaviour.[15] Similarly, while coordination chemistry has proven to be key in the design of ligands that generate the right splitting among the d-based molecular orbitals for the molecule to exhibit SCO, organometallic molecules usually have a larger ligand-field splitting that leads to low-spin states, and very few examples have been reported.[16,17] Among the few organometallic SCO systems reported, the manganocene family ([$Mn(Cp^R)_2$]) has provided several examples of functionalized molecules exhibiting such behaviour.[17-20] More relevant is the fact that the transition temperature ($T_{1/2}$), defined as the temperature with equal populations of both spin-states and a key physical property in SCO systems, can be modulated in such families via the R group. The interplay between steric and electronic effects in tuning $T_{1/2}$ for the alkyl substituted manganocenes of general formula [$Mn(Cp^{n-R})_2$] (n = 1 to 5 and R = Me, ^iPr or ^tBu) has been analyzed by means of computational studies.[21] That work showed that

the ligand field around the Mn^{II} ion can be increased by adding more electron-donor groups, such as methyl, but that bulky substituents, such as *iso*-propyl or *tert*-butyl, can have the opposite effect due to the steric hindrance that they introduce in the molecule, which pushes the Cp rings away from the metal center. However, the effect of the functionalization of the cyclopentadienyl ligand with other groups than methyl in order to control the SCO properties of the $[Mn(Cp^{1-R})_2]$ family has not been explored. In this work, we used electronic structure calculations at the density functional theory (DFT) level to evaluate the effect that different R groups have over the transition temperature ($T_{1/2}$). By changing the R group we will show that a fine degree of tuning over $T_{1/2}$ can be achieved, allowing for the modulation of such value in a wide range of temperatures. The presented results open the door to *in silico* design of new metallocenes with selected SCO properties, thus providing experimental chemists a powerful tool for the rational design of new molecules with specific transition temperatures.

Computational Details:

All density functional calculations (DFT) have been carried out with Gaussian 09 (revision D)[22] except those with the SCAN functional, which have been performed using the Q-Chem 5.0 electronic structure suite.[23] All calculations have been converged to 10^{-8} for the density matrix elements, and the corresponding vibrational analysis was done to ensure that they were minima along the potential energy surface. The fully optimized basis set from Ahlrichs and co-workers,[24] including polarization functions, was employed for all atoms. In particular, five different basis set schemes were tested during the benchmarking process: TZV for all elements (BS1), TZVP for manganese and TZV for the rest (BS2), TZVP for all elements (BS3), QZVP for manganese and TZVP for the rest (BS4) and QZVP for all elements (BS5) (see results section and Supporting Information). To compute the transition temperatures, several post pro-

cessing scripts were used (see Supporting Information). The *n*-electron valence per-turbation theory (NEVPT2)[25] calculations were performed with the Orca 4.0 code.[26] In these calculations, we employed the def2TZVPP basis set, including the corresponding auxiliary basis set for the correlation and Coulomb fitting. The active space contains the 5 d-orbitals of the metal and 4 electrons, and the *ab initio* ligand-field theory (AILFT) approach was employed to extract the related orbitals.[27]

2. Results

Previous work on the computational modeling of $T_{1/2}$ in $[Mn(Cp^R)_2]$ (R = Me, ^{i}Pr or ^{t}Bu) showed that DFT methods (OPBE in particular) were able to correctly model the SCO behaviour in such systems.[21] However, we decide to pursue a systematic bench-mark of different DFT methods aiming to be as quantitative as possible towards the calculation of the transition temperature. With that goal, we choose as a benchmark model the $[Mn(Cp^{1-Me})_2]$ system for its simplicity, which allows the testing of multiple functionals and basis set schemes, and also because there is structural information in gas phase (d(Mn-C) = 2.433 Å and 2.144 Å for high- and low-spin respectively),[28] as well as a proper characterization of its $T_{1/2}$ (303 K),[17] data that will allow us to properly calibrate the computational method of choice.

Several DFT methods were tested for the $[Mn(Cp^{1-Me})_2]$ system, including TPSSh,[29,30] OPBE,[31,32] OLYP,[31,33] M06L,[34] B3LYP,[35] B3LYP*[36] and SCAN.[37] A full optimization in both high- and low-spin state using BS3 was done, followed by the corresponding vibrational analysis to ensure its minimum nature. The corresponding spin-state energy differences as well as relevant geometric parameters and the calculated $T_{1/2}$ (where meaningful) are given in table 1.

Table 1: Spin-state energy gap for the $[Mn(Cp^{1-Me})_2]$ system using different DFT methods, as well as the average Mn-C bond length. All distances are in Å, energies in kcal/mol and temperatures in K.

Method	d(Mn-C) (S=5/2)	d(Mn-C) (S=1/2)	$\Delta E_{(HS-LS)}$	$T_{1/2}$
TPSSh	2.392	2.125	11.21	527
OPBE	2.381	2.089	9.25	423
OLYP	2.417	2.127	4.68	193
B3LYP	2.421	2.163	−4.97	-
B3LYP*	2.448	2.135	−9.42	-
M06L	2.373	2.097	−1.67	-
SCAN	2.383	2.117	5.05	755

As can be seen from table 1, TPSSh, OBPE, OLYP and SCAN all correctly predict the low-spin state as the ground state. Particularly, OLYP provides with accurate Mn-C bond lengths compared with the experimental values as well as an appropriate energy gap for SCO to occur. Among the most promising methods, a systematic exploration of the basis set effect was carried out. A total of five different basis set schemes were tested (BS1 to BS5, see computational details). The results are summarized in Table 2.

As can be seen from table 2, several combinations achieve a remarkable precision when computing the experimental transition temperature ($T_{1/2}$ = 303 K), as has been previously reported.[21,38] An optimal balance between computational cost and accuracy can be achieved using OLYP/BS4. The same is observed by analyzing the metal-ligand bond lengths (see Supporting Information), as Mn-C bond lengths are in excellent agreement with the experimental data (d(Mn-C) = 2.409 and 2.121 Å for high and

low-spin, respectively). Slightly better results are obtained with OLYP/BS5, but the computational cost increases by a factor of 10. Thus, for the rest of this work we will use OLYP/BS4 as a method.

Table 2: Computed spin-state energy differences (ΔE) and transition temperatures ($T_{1/2}$) for the $[Mn(Cp^{1\text{-Me}})_2]$ system using different DFT methods. All energies are in kcal/mol and all temperatures in K.

	TPSSh		OPBE		OLYP		SCAN		B3LYP*	
	ΔE	$T_{1/2}$	ΔE	$T_{1/2}$	ΔE	$T_{1/2}$	ΔE	$T_{1/2}$	ΔE	$T_{1/2}$
BS1	7.83	269	1.66	215	6.00	21	2.08	157	−12.89	-
BS2	8.31	380	1.53	255	5.65	41	1.60	144	−12.81	-
BS3	11.21	527	4.68	423	9.25	193	5.05	451	−9.42	-
BS4	13.06	601	6.05	482	11.18	274	7.24	623	5.39	219
BS5	14.10	634	7.29	537	12.64	320	8.38	755	6.14	385

Previously, we showed that in the $[Mn(Cp^{n\text{-Me}})_2]$ family (n = 0 to 5), it is possible to tune the ligand field via ring functionalization.[21] Adding more methyl groups to the cyclopentadienyl ring increases the gap between the non-bonding and antibonding orbitals, switching from spin-crossover systems, such as $[Mn(Cp)_2]$ or $[Mn(Cp^{1\text{-Me}})_2]$, to low-spin systems, like $[Mn(Cp^*)_2]$, as experimentally observed. This effect in the spin-state energy gap is purely electronic, because the geometrical data of the $[Mn(Cp^{n\text{-Me}})_2]$ systems barely changes from the naked cyclopentadienyl to the pentamethylcyclopentadienyl. Motivated by such results, we decided to explore the electronic effect of different substituents in the Cp ring on the spin-crossover behaviour in $[Mn(Cp^{1\text{-R}})_2]$ systems. To explore such behaviour, we conducted a search in the Cam-

bridge Structural Database (CSD v5.41)[39] for monosubstituted $[M(Cp^{1-R})_2]$ systems (M=Cr, Mn, Fe, Co or Ni), in order to check for different functionalizations in the Cp ring experimentally reported (see ESI). For each one of this functionalized Cp rings, we built the corresponding $[Mn(Cp^{1-R})_2]$ molecule, and computed the corresponding ΔE and $T_{1/2}$. The results are summarized in Table 3.

Table 3: Computed ΔE and $T_{1/2}$ for $[Mn(Cp^{1-R})_2]$ systems studied in this work. For each R group, we included the corresponding set of Hammett parameters. d corresponds to the average Mn-cyclopentadiene ring centroid-distance in both spin states. All energies are in kcal/mol, distances in Å and temperatures in K.

Substituent (R)	σ_{meta}	σ_{para}	ΔE	$T_{1/2}$	d_{LS}	d_{HS}
NH$_2$	−0.16	−0.66	9.91	452	1.740	2.103
Me	−0.07	−0.17	6.05	274	1.739	2.102
(NH)(CO)OMe	−0.02	−0.17	6.30	292	1.733	2.108
SiMe$_3$	−0.04	−0.07	3.10	143	1.730	2.083
B(OH)$_2$	−0.01	0.12	3.08	133	1.724	2.078
C(H)(Me)(OH)	0.08	−0.07	4.90	274	1.739	2.086
CCPh	0.14	0.16	1.11	38	1.738	2.086
I	0.18	0.18	6.10	281	1.728	2.094
(CH)NOH	0.22	0.10	0.90	26	1.733	2.086
SPh	0.23	0.07	4.77	195	1.733	2.089
NCO	0.27	0.19	4.13	200	1.734	2.103
F	0.34	0.06	6.71	336	1.729	2.094
N$_3$	0.37	0.08	4.38	194	1.734	2.102
Cl	0.37	0.23	4.55	226	1.731	2.100

Substituent (R)	σ_{meta}	σ_{para}	ΔE	$T_{1/2}$	d_{LS}	d_{HS}
(CO)Me	0.38	0.50	1.60	62	1.724	2.081
Br	0.39	0.23	4.81	202	1.733	2.099
PCl_2	0.54	0.61	4.57	182	1.736	2.091
CN	0.56	0.66	0.98	33	1.739	2.092
NO_2	0.71	0.78	1.22	31	1.739	2.089
$SOCl_2$	1.20	1.11	4.16	194	1.736	2.090

As can be seen from Table 3, in the low-spin state, the average value for d(Mn-Cp) remains almost unaltered, with an average value of (1.740 ± 0.002) Å (95% confidence). The same trend is observed for the high-spin state as well ((2.090 ± 0.004) Å, 95% confidence). However, although the geometry remains almost identical, large changes in the spin-state energy gap as well as the $T_{1/2}$ are observed. These changes can therefore only be attributed to the changes in the electronic structure of the $[Mn(Cp^{1-R})_2]$ system introduced by the R group.

In Figure 1, we plotted the computed $T_{1/2}$ against the σ_p Hammett parameter[40] for all the $[Mn(Cp^{1-R})_2]$ systems in Table 3. As can be seen in the figure, a trend with the electron donating (or electron withdrawing) character of the R group can be observed. In general, a decrease in the $T_{1/2}$ is observed with increasingly withdrawing character of the R group. Although this trend in the computed $T_{1/2}$ spans on a 500 K range, the geometries of the computed systems remains almost identical, as can be observed using the average Mn-Cp centroid-distance. For all systems in Table 3, this parameter has average values of 1.734 Å and 2.092 Å for the low- and high-spin states, respectively (standard deviations of 0.0047 and 0.0082, see Supporting Information). This

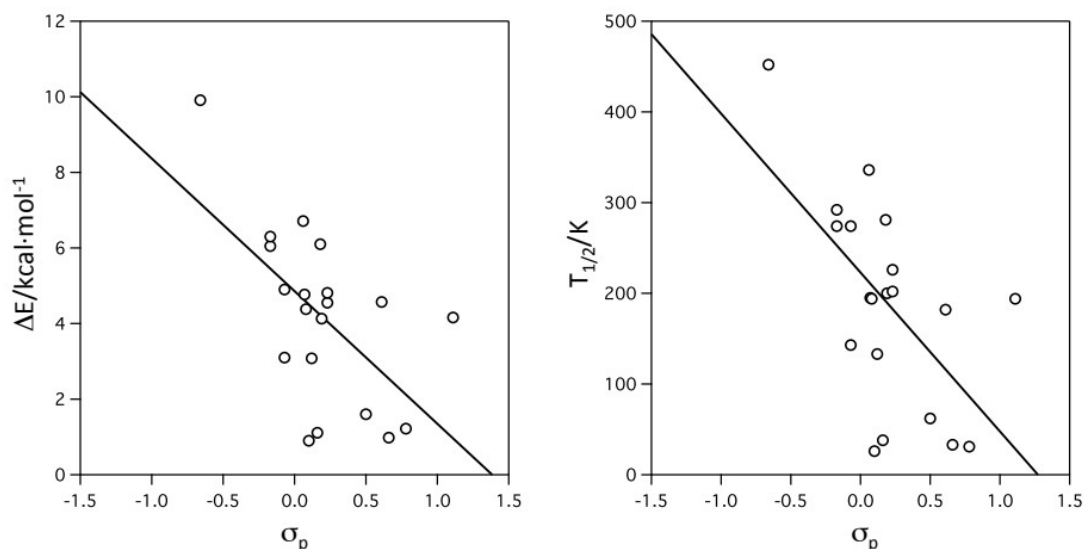clearly shows the electronic nature of the tuning effect that the R group has on the SCO properties of the [Mn(Cp^R)$_2$] family.

Figure 1: Computed ΔE and $T_{1/2}$ for the studied [Mn(Cp$^{1\text{-}R}$)$_2$] systems against the σ_p Hammett parameter ($R^2 = 0.35$ and 0.38). All energies are in kcal/mol and temperatures in K.

This data shows that there is a way to tune the spin-state gap in [Mn(Cp^R)$_2$] systems via ligand functionalization, and that it is possible to adjust such gap to tune the $T_{1/2}$ up or down. Motivated by such results, we decide to explore the possibility of designing new SCO systems among the other metallocenes which can, in principle, exhibit such behaviour. First, we computed the spin-state energy gap for the [M(Cp$^{1\text{-}Me}$)$_2$] family (M = Cr^{II}, Mn^{II}, Fe^{II} and Co^{II}). The computed energy gaps are in all cases larger than for the [Mn(Cp$^{1\text{-}Me}$)$_2$] case (see Supporting Information), but the [Cr(Cp$^{1\text{-}Me}$)$_2$] is close enough so one can envision a tuning of the ligand field to achieve SCO. Therefore, we replaced the methyl group by electron withdrawing groups (R=NO$_2$ and CN) to see if we can tune down the spin-state energy gap to a range where SCO can occur. Results for such calculations are summarized in Table 4.

Table 4: Computed energy spin-state differences for $[Cr(Cp^{1-R})_2]$ (R=Me, NO_2 and CN), together with the corresponding ΔH, ΔS and calculated $T_{1/2}$.

Substituent (R)	ΔE/kcal mol^{-1}	ΔH/kcal mol^{-1}	ΔS/cal K^{-1} mol^{-1}	$T_{1/2}$/K
R = Me	9.85	9.50	11.61	818
R = NO_2	6.49	6.21	7.02	885
R = CN	7.72	7.46	7.50	994

Although these substituents have a similar effect on the $[Cr(Cp^{1-R})_2]$ as the one observed in $[Mn(Cp^{1-R})_2]$, i. e. they reduce the spin-state energy gap, the corresponding $T_{1/2}$ does not experience a significant decrease. To understand that behaviour, we must analyze the corresponding entropy change in both families. While for the $[Mn(Cp^{1-Me})_2]$ ΔS = 19.87 cal K^{-1} mol^{-1}, for the chromium analog $[Cr(Cp^{1-Me})_2]$ this value is only ΔS = 11.61 cal K^{-1} mol^{-1}. This reduction of the entropy change is largely due to the electronic contribution to the entropy change, ΔS_{elec}, that can be calculated as $\Delta S_{elec} = R \cdot \dfrac{2 \cdot S_{HS} + 1}{2 \cdot S_{LS} + 1}$. For Mn^{II}, there is a large change in the total spin between high-spin and low-spin states (S_{HS} = 5/2, S_{LS} = 1/2), but for Cr^{II}, the situation is much softer. Actually, the computed ΔS_{elec} for Mn^{II} and Cr^{II} are, respectively, 5.96 and 3.31 cal K^{-1} mol^{-1}. Because $T_{1/2} = \Delta H/\Delta S$, for the chromium systems, the reduction of the spin-state energy gap is largely compensated by the decrease in the entropy change due to the Cr^{II} electron configuration. Nevertheless, if we can reduce the ΔH even more for a $[Cr(Cp^{1-R})_2]$ system, it should, potentially, exhibit SCO behaviour. Following this idea, we introduced a second NO_2 substituent, and computed the spin-state energy gap for the $[Cr(Cp^{1,3-NO_2})_2]$ molecule. For that molecule,

ΔH=3.62 kcal mol^{-1} and ΔS = 10.0 cal K^{-1} mol^{-1}, thus making its $T_{1/2}$ = 362 K, a value

that makes it a potential candidate for exhibiting SCO behaviour.

3. Discussion

Our working hypothesis is that, in principle, one can tune the ligand field around the

metal center by making the ring more negatively charged, as is experimentally ob-

served when moving from [Mn(Cp$^{1\text{-Me}}$)$_2$], an SCO molecule, to the fully methylated

system [Mn(Cp*)$_2$], a low-spin system.[21] Following this idea, different substituents

with more or less electron withdrawing effects have been tested in the [Mn(Cp$^{1\text{-R}}$)$_2$]

system. Although a trend is observed, the results are far from showing a clear correla-

tion between the computed $T_{1/2}$ and the Hammett parameter σ_p. However, a look at

figure 1 allows us to identify several outliers that greatly deviate from the trend.

These are R=SO$_2$Cl, CCPh, SiMe$_3$, (CH)NOH, B(OH)$_2$ and PCl$_2$. Without such points,

the correlation becomes much more clear, as can be seen in Figure 2.

We can thus see that the use of the Hammett parameters to describe the electron-do-

nating character of the substituents and its effect on tuning $T_{1/2}$ holds to a great extent,

but some points are clearly out of the trend. To understand the origin of such devia-

tions, we collected more data on the low-spin state systems. In particular, NEVPT2

calculations analyzed using the *ab initio* ligand field theory (AILFT) framework were

used to get the energies of the five d-based molecular orbitals, and a Hirshfeld charge

analysis was done to calculate the total charge of the Cp$^{1\text{-R}}$ rings for each R. Numeri-
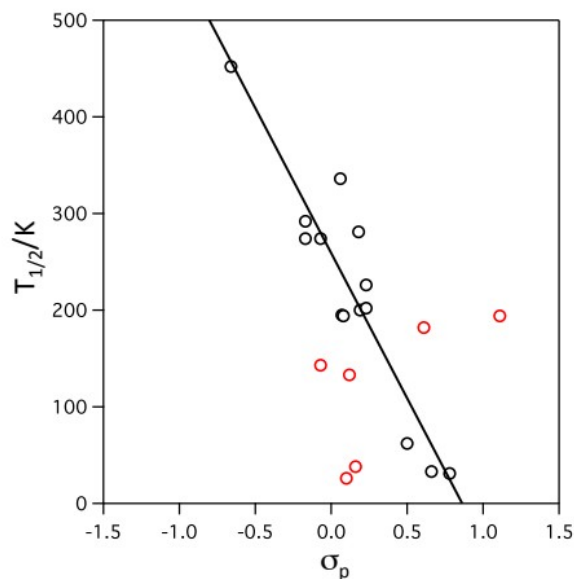
cal data can be found in the SI.

Figure 2: Computed $T_{1/2}$ for the $[Mn(Cp^{1-R})_2]$ studied systems against the σ_p Hammett parameter ($R^2 = 0.86$). Marked in red are the outliers from the trend. All temperatures are in K.

Let's first analyze the Cp^{1-R} ring charge. A correlation can be found between the σ_p Hammett parameter and the total charge of the ring ($R^2 = 0.74$, see SI). However, a close inspection of the numerical data shows that $SiMe_3$ produces an unusually positive charge on the ligand, falling off the expected trend. In fact, removing that point greatly increases the correlation between charge and σ_p ($R^2 = 0.85$). This result shows that the Hammett parameter is mostly reflecting the total charge of the ring and its effect on the splitting of the d-based molecular orbitals, but may be missing other orbital effects that can be at play. In fact, the numerical data for the outliers shows that they tend to have smaller ligand-field splitting energy gaps than expected. To further analyze the orbital effect, we compared the frontier molecular orbitals of a pure σ-donor ligand ($R=CH_3$) with the ones from $R = SO_2Cl$, CCPh, (CH)NOH, $B(OH)_2$ and PCl_2. The possibility of extending the π-system of the ligand over the R group reduces

the antibonding character of the d_{xy} (or d_{yx}) orbitals, thus lowering its energy and producing HOMO-LUMO gaps smaller than expected.

4. Conclusions

In this work, we presented a robust computational methodology to study the spin-crossover behaviour of manganocenes of general formula $[Mn(Cp^{1-R})_2]$. The combination of the OLYP exchange correlation functional with a triple-ζ basis set with polarization functions on all atoms provides a computed $T_{1/2}$ in excellent agreement with the available experimental data for the $[Mn(Cp^{1-Me})_2]$ system. Also, geometrical parameters are properly reproduced. Single functionalization of the cyclopentadienyl ring allows for a fine-tuning of the SCO properties in this family. A general trend is observed with the electron-donating character of the R group. In general, the more electron-donating the R group is, the higher the $T_{1/2}$. The electronic modulating effect of the R group is validated by the almost non-existing changes in the geometries of the studied systems, all of them having a very similar Mn-Cp distance in both spin-states. The use of R groups to increase or decrease the transition temperature opens the door for the use of other metals aside from manganese, which so far is the only one able to exhibit SCO in metallocenes. In particular, we showed that chromocene has a spin-state energy gap that can, in principle, be tuned using electron-withdrawing R groups such as CN or NO_2. Although single functionalization of the Cp ring with such substituents does indeed reduce the spin-state energy gap, it is not enough to achieve a reasonable $T_{1/2}$ due to the much lower electronic entropic contribution from Cr^{II} compared to the one provided by Mn^{II}. However, this can be bypassed by introducing a second NO_2 group to the ring. Thus, our calculations not only allow for a rational understanding on how to tune the SCO properties of the $[Mn(Cp^{1-R})_2]$ family,

but also open the door for the computational design of new metallocenes with tailored spin-crossover properties that expand the current library of such compounds.

Author information:

florian.matz@pci.uni-hannover.de

jordi.cirera@qi.ub.es

Notes: The authors declare no competing financial interest.

References:

1   M. A. Halcrow, *Spin-Crossover Materials: Properties and Applications*, 2013.

2   P. Gütlich and H. A. Goodwin, 2012, pp. 1–47.

3   P. Gütlich, A. B. Gaspar and Y. Garcia, *Beilstein J. Org. Chem.*, 2013, **9**, 342–391.

4   P. Gütlich and H. A. Goodwin, *Spin Crossover in Transition Metal Compounds III*, Springer Berlin Heidelberg, Berlin, Heidelberg, 2004, vol. 235.

5   D. Aravena and E. Ruiz, *J. Am. Chem. Soc.*, 2012, **134**, 777–779.

6   T. Mahfoud, G. Molnár, S. Cobo, L. Salmon, C. Thibault, C. Vieu, P. Demont and A. Bousseksou, *Appl. Phys. Lett.*, 2011, **99**, 053307.

7   V. Meded, A. Bagrets, K. Fink, R. Chandrasekar, M. Ruben, F. Evers, A.

Bernand-Mantel, J. S. Seldenthuis, A. Beukman and H. S. J. van der Zant, *Phys. Rev. B*, 2011, **83**, 245415.

8   F. Prins, M. Monrabal-Capilla, E. A. Osorio, E. Coronado and H. S. J. van der Zant, *Adv. Mater.*, 2011, **23**, 1545–1549.

9   L. Cambi and L. Szegö, *Berichte der Dtsch. Chem. Gesellschaft (A B Ser.*, 1931, **64**, 2591–2598.

10   R. W. Hogue, S. Singh and S. Brooker, *Chem. Soc. Rev.*, 2018.

11   H. S. Scott, R. W. Staniland and P. E. Kruger, *Coord. Chem. Rev.*, 2018.

12   K. Senthil Kumar and M. Ruben, *Coord. Chem. Rev.*, 2017.

13   G. A. Craig, O. Roubeau and G. Aromí, *Coord. Chem. Rev.*, 2014.

14   P. Gütlich, Y. Garcia and H. A. Goodwin, *Chem. Soc. Rev.*, 2000, **29**, 419–427.

15   J. Olguín, *Coord. Chem. Rev.*, 2020, **407**, 213148.

16   H.-J. Lin, D. Siretanu, D. A. Dickie, D. Subedi, J. J. Scepaniak, D. Mitcov, R. Clérac and J. M. Smith, *J. Am. Chem. Soc.*, 2014, **136**, 13326–13332.

17   M. E. Switzer, R. Wang, M. F. Rettig and A. H. Maki, *J. Am. Chem. Soc.*, 1974, **96**, 7669–7674.

18   M. D. Walter, C. D. Sofield, C. H. Booth and R. A. Andersen, *Organometallics*, 2009, **28**, 2005–2019.

19   M. L. Hays and T. P. Hanusa, in *Advances in Organometallic Chemistry*, 1996, vol. 40, pp. 117–170.

20   M. L. Hays, D. J. Burkey, J. S. Overby, T. P. Hanusa, S. P. Sellers, G. T. Yee and V. G. Young, *Organometallics*, 1998, **17**, 5521–5527.

21   J. Cirera and E. Ruiz, *Inorg. Chem.*, 2018, **57**, 702–709.

22   M. J. Frisch, G. W. Trucks, H. B. Schlegel, G. E. Scuseria, M. A. Robb, J. R. Cheeseman, G. Scalmani, V. Barone, B. Mennucci, G. A. Petersson, H. Nakat-

suji, M. Caricato, X. Li, H. P. Hratchian, A. F. Izmaylov, J. Bloino, G. Zheng, J. L. Sonnenberg, M. Hada, M. Ehara, K. Toyota, R. Fukuda, J. Hasegawa, M. Ishida, T. Nakajima, Y. Honda, O. Kitao, H. Nakai, T. Vreven, J. A. Montgomery Jr., J. E. Peralta, F. Ogliaro, M. J. Bearpark, J. Heyd, E. N. Brothers, K. N. Kudin, V. N. Staroverov, R. Kobayashi, J. Normand, K. Raghavachari, A. P. Rendell, J. C. Burant, S. S. Iyengar, J. Tomasi, M. Cossi, N. Rega, N. J. Millam, M. Klene, J. E. Knox, J. B. Cross, V. Bakken, C. Adamo, J. Jaramillo, R. Gomperts, R. E. Stratmann, O. Yazyev, A. J. Austin, R. Cammi, C. Pomelli, J. W. Ochterski, R. L. Martin, K. Morokuma, V. G. Zakrzewski, G. A. Voth, P. Salvador, J. J. Dannenberg, S. Dapprich, A. D. Daniels, Ö. Farkas, J. B. Foresman, J. V Ortiz, J. Cioslowski and D. J. Fox, *Gaussian 09, Rev. D01*.

23 Y. Shao, Z. Gan, E. Epifanovsky, A. T. B. Gilbert, M. Wormit, J. Kussmann, A. W. Lange, A. Behn, J. Deng, X. Feng, D. Ghosh, M. Goldey, P. R. Horn, L. D. Jacobson, I. Kaliman, R. Z. Khaliullin, T. Kuš, A. Landau, J. Liu, E. I. Proynov, Y. M. Rhee, R. M. Richard, M. A. Rohrdanz, R. P. Steele, E. J. Sundstrom, H. L. Woodcock, P. M. Zimmerman, D. Zuev, B. Albrecht, E. Alguire, B. Austin, G. J. O. Beran, Y. A. Bernard, E. Berquist, K. Brandhorst, K. B. Bravaya, S. T. Brown, D. Casanova, C. M. Chang, Y. Chen, S. H. Chien, K. D. Closser, D. L. Crittenden, M. Diedenhofen, R. A. Distasio, H. Do, A. D. Dutoi, R. G. Edgar, S. Fatehi, L. Fusti-Molnar, A. Ghysels, A. Golubeva-Zadorozhnaya, J. Gomes, M. W. D. Hanson-Heine, P. H. P. Harbach, A. W. Hauser, E. G. Hohenstein, Z. C. Holden, T. C. Jagau, H. Ji, B. Kaduk, K. Khistyaev, J. Kim, J. Kim, R. A. King, P. Klunzinger, D. Kosenkov, T. Kowalczyk, C. M. Krauter, K. U. Lao, A. D. Laurent, K. V. Lawler, S. V. Levchenko, C. Y. Lin, F. Liu, E. Livshits, R. C. Lochan, A. Luenser, P. Manohar, S. F. Manzer, S. P.

Mao, N. Mardirossian, A. V. Marenich, S. A. Maurer, N. J. Mayhall, E. Neuscamman, C. M. Oana, R. Olivares-Amaya, D. P. Oneill, J. A. Parkhill, T. M. Perrine, R. Peverati, A. Prociuk, D. R. Rehn, E. Rosta, N. J. Russ, S. M. Sharada, S. Sharma, D. W. Small, A. Sodt, T. Stein, D. Stück, Y. C. Su, A. J. W. Thom, T. Tsuchimochi, V. Vanovschi, L. Vogt, O. Vydrov, T. Wang, M. A. Watson, J. Wenzel, A. White, C. F. Williams, J. Yang, S. Yeganeh, S. R. Yost, Z. Q. You, I. Y. Zhang, X. Zhang, Y. Zhao, B. R. Brooks, G. K. L. Chan, D. M. Chipman, C. J. Cramer, W. A. Goddard, M. S. Gordon, W. J. Hehre, A. Klamt, H. F. Schaefer, M. W. Schmidt, C. D. Sherrill, D. G. Truhlar, A. Warshel, X. Xu, A. Aspuru-Guzik, R. Baer, A. T. Bell, N. A. Besley, J. Da Chai, A. Dreuw, B. D. Dunietz, T. R. Furlani, S. R. Gwaltney, C. P. Hsu, Y. Jung, J. Kong, D. S. Lambrecht, W. Liang, C. Ochsenfeld, V. A. Rassolov, L. V. Slipchenko, J. E. Subotnik, T. Van Voorhis, J. M. Herbert, A. I. Krylov, P. M. W. Gill and M. Head-Gordon, *Mol. Phys.*, 2015, **113**, 184–215.

24   A. Schafer, C. Huber and R. Ahlrichs, *J. Chem. Phys.*, 1994, **100**, 5829–5835.

25   C. Angeli, R. Cimiraglia and J. P. Malrieu, *J. Chem. Phys.*, 2002, **117**, 9138–9153.

26   F. Neese, *WIREs Comput. Mol. Sci.*, 2018, **8**, e1327.

27   S. K. Singh, J. Eng, M. Atanasov and F. Neese, *Coord. Chem. Rev.*, 2017, 344, 2–25.

28   A. Almenningen, A. Haaland and S. Samdal, *J. Organomet. Chem.*, 1978, **149**, 219–229.

29   J. M. Tao, J. P. Perdew, V. N. Staroverov and G. E. Scuseria, *Phys. Rev. Lett.*, 2003, **91**, 146401.

30   V. N. Staroverov, G. E. Scuseria, J. M. Tao and J. P. Perdew, *J. Chem. Phys.*,

2003, **119**, 12129–12137.

31   N. C. Handy and A. J. Cohen, *Mol. Phys.*, 2001, **99**, 403–412.

32   J. P. Perdew, K. Burke and M. Ernzerhof, *Phys. Rev. Lett.*, 1996, **77**, 3865–
      3868.

33   C. Lee, W. Yang and R. G. Parr, *Phys. Rev. B*, 1988, **37**, 785–789.

34   Y. Zhao and D. G. Truhlar, *J. Chem. Phys.*, 2006, **125**, 194101.

35   A. D. Becke, *J. Chem. Phys.*, 1993, **98**, 5648–5652.

36   M. Reiher, O. Salomon and B. A. Hess, *Theor. Chem. Acc.*, 2001, **107**, 48–55.

37   J. Sun, A. Ruzsinszky and J. Perdew, *Phys. Rev. Lett.*, 2015, **115**, 036402.

38   J. Cirera, M. Via-Nadal and E. Ruiz, *Inorg. Chem.*, 2018, **57**, 14097–14105.

39   C. R. Groom, I. J. Bruno, M. P. Lightfoot and S. C. Ward, *Acta Crystallogr.
      Sect. B Struct. Sci. Cryst. Eng. Mater.*, 2016, **72**, 171–179.

40   C. Hansch, A. Leo and R. W. Taft, *Chem. Rev.*, 1991, **91**, 165–195.